Breast Cancer Research and Treatment (2019) 174:669–677
https://doi.org/10.1007/s10549-018-05122-7

PRECLINICAL STUDY

# Three-dimensional tumor visualization of invasive breast carcinomas using whole-mount serial section histopathology: implications for tumor size assessment

G. M. Clarke[1] · C. M. B. Holloway[2,3] · J. T. Zubovits[4,5] · S. Nofech-Mozes[4,6] · M. Murray[7] · K. Liu[8] · D. Wang[8] · A. Kiss[9,10] · M. J. Yaffe[11,12]

Received: 26 June 2018 / Accepted: 26 December 2018 / Published online: 5 January 2019
© Springer Science+Business Media, LLC, part of Springer Nature 2019

## Abstract

**Purpose** Linear tumor size (T-size) estimated with conventional histology informs breast cancer management. Previously we demonstrated significant differences in margin and focality estimates using conventional histology versus digital whole-mount serial sections (WMSS). Using WMSS we can measure T-size or volume. Here, we compare WMSS T-size with volume, and with T-size measured conventionally. We also compare the ellipsoid model for calculating tumor volume to direct, WMSS measurement.

**Methods** Two pathologists contoured regions of invasive carcinoma and measured T-size from both WMSS and (simulated) conventional sections in 55 consecutive lumpectomy specimens. Volume was measured directly from the contours. Measurements were compared using the paired *t*-test or Spearman's rank-order correlation. A five-point 'border index' was devised and assigned to each case to parametrize tumor shape considering 'compactness' or cellularity. Tumor volumes calculated assuming ellipsoid geometry were compared with direct, WMSS measurements.

**Results** WMSS reported significantly larger T-size than conventional histology in the majority of cases [61.8%, 34/55; means = (2.34 cm; 1.99 cm), $p < 0.001$], with a 16.4% (9/55) rate of 'upstaging'. The majority of discordances were due to undersampling. T-size and volume were strongly correlated ($r = 0.838$, $p < 0.001$). Significantly lower volume was obtained with WMSS versus ellipsoid modeling [means = (1.18 $cm^3$; 1.45 $cm^3$), $p < 0.001$].

**Conclusions** Significantly larger T-size is measured with WMSS than conventionally, due primarily to undersampling in the latter. Volume and linear size are highly correlated. Diffuse tumors interspersed with normal or non-invasive elements may be sampled less extensively than more localized masses. The ellipsoid model overestimates tumor volume.

**Keywords** Breast cancer · Lumpectomy · Whole-mount serial sections · Large-format histology · Histologic size · Tumor volume

## Abbreviations

| | |
|---|---|
| TNM | Tumor Node Metastasis |
| AJCC/UICC | American Joint Committee on Cancer/ Union for International Cancer Control |
| 3-D | Three-dimensional |
| WMSS | Whole-mount serial sections |
| WM | Whole-mount |
| H&E | Hematoxylin and eosin |
| SCS | Simulated conventional sections |
| AP | Anterior–posterior |
| SI | Superior–inferior |
| ML | Medial–lateral |
| BI | Border Index |

✉ M. J. Yaffe
martin.yaffe@sunnybrook.ca

Extended author information available on the last page of the article

## Introduction

Tumor size is an established prognostic factor in breast cancer management [1–4]. It is a key component of the TNM staging system, correlating strongly with lymph node involvement, and is frequently used to guide treatment decisions [5–8].

Histologic tumor size is measured from the surgical specimen, by directed sampling which is guided by imaging and gross examination [9]. The greatest linear dimension is reported as 'T-size' [5]. Artifacts can result from inadequate

or unrepresentative sampling, or inaccurate preservation of specimen conformation and orientation. Inaccurate estimates of margin width and tumor size may result [10, 11].

T-size may fail to accurately reflect tumor burden. Theoretical models have shown that metastatic potential depends on the total number of cells and the probability of each to disseminate [12]. Tumors may invade the surrounding stroma via dense sheets or sparsely distributed single cells, yielding a widely variable number of cancer cells per volume of breast tissue [13]. The tumor-to-stroma ratio may also be an important prognostic variable for primary invasive carcinoma [14–16], further challenging the concept of a unidimensional surrogate for tumor size.

There is renewed interest in three-dimensional (3-D) histologic tumor attributes such as volume and shape. To date, there are no compelling data showing a difference in outcome prediction for breast tumors when measured by volume versus linear size [17]. However a significant association between tumor volume and both overall and disease-free survival, or prediction of lymph node metastasis, has been shown for other tumor sites [18–20]. While such studies underscore the clinical importance of 3-D measurements, they share two common methodological limitations: using conventional histology, the linear measurements are based on a limited sampling, and the volume calculations rely on assumptions regarding shape.

We have developed a digital whole-mount serial section (WMSS) platform for improved 3-D histologic evaluation of breast lumpectomy specimens, and demonstrated whole-tumor volume renderings [21, 22]. Whole-mount serial sections reduce sampling bias by capturing an entire cross-sectional area on each slide, serially throughout the entire specimen. This approach increases detection sensitivity for involved margins and multifocality, compared with conventional histology [11]. WMSS provides an ideal platform for assessing tumor size because linear measurements are unbiased by conventional sampling effects or sparse sectioning, and volumetric measurements are unbiased by the choice of geometric model characterizing the underlying tumor distribution.

We conducted a study to compare T-size measured by WMSS versus conventional assessment, and also compare linear versus volumetric size. We also assessed the influence of both sampling effects and 3-D shape in the context of cellularity. Finally, we compared calculated versus directly-measured tumor volume, using the ellipsoid model and WMSS respectively.

## Methods

### Specimen and image preparation

The study was conducted using lumpectomy specimens obtained from the Department of Anatomic Pathology at Sunnybrook Health Sciences Centre. Sunnybrook's institutional Research Ethics Board approved the study (ID 192-2009) and waived the requirement for obtaining patient consent. The study included consecutive breast-conserving surgeries performed from November 2009 to November 2011 and included biopsy-confirmed carcinoma of any histologic type.

Fifty-five patients were included in the study, out of a total of 90 who were assessed for eligibility. The following exclusion criteria were applied: patients who received preoperative systemic or radiation therapy (13); specimens that would have been sampled in toto at the time of gross specimen preparation or where intra-operative consultation was required (2,9) ; cases where the final diagnosis was ductal or lobular carcinoma in situ (3). Seven cases were excluded due to workflow constraints, and one for cancelation of surgery post-inclusion.

The WMSS specimen preparation and processing techniques have been described elsewhere [22, 23]. Briefly, the entire surgical specimen is suspended in a density-matched gel to preserve conformation during serial, whole-mount (WM) slicing at uniform 0.4 cm intervals from medial to lateral aspect in a custom mould. The slices are formalin-fixed, microwave processed, and embedded into paraffin blocks. One WM section is prepared from the top of each block, stained and digitized at 2 μm/pixel resolution as deemed to be adequate for detection of abnormality [24, 25].

Specimens included in this study were processed to produce intact whole-mount sections, and, therefore, the conventional sections were digitally simulated for each case. The simulated conventional sections (SCS) represent the tissues that would be available for pathologist interpretation had the standard assessment been performed [11]. The pathologist assistant identified regions of tissue that would be sampled in the conventional approach based on inspection of the WM slices, and created 'virtual samples' or simulated blocks by digitally outlining these regions on optical images of the formalin-fixed slices. These virtual samples were transposed to the corresponding areas on the digitized, high-resolution WMSS images, which were then cropped to create the set of SCS for each case. The optical images were also used to simulate the specimen grossing diagram that would be available to help the pathologist orient the samples in conventional workflow.

### Pathologist assessment and measurement of T-size and tumor volume

The primary metrics, WMSS T-size, SCS T-size, and WMSS tumor volume, were obtained as follows:

The WMSS images were assessed by two pathologists (KL, JZ) who identified areas of invasive disease with digital

contours on the computer image display program Sedeen (v.4.2.3, Pathcore Inc., Toronto, Canada). The contour coordinates were captured in .xml ('extensible markup language') format and imported into MATLAB (MATLAB 8.6.0.26724 (R2015b); Math Works Inc; Natick MA, USA) for use in calculating the enclosed tumor area. In the absence of CAP/ASCO guidelines for measuring tumor volume, WMSS volume was calculated using a Riemann summation approach, multiplying the total area computed in each WM image assigned to the largest invasive focus by the nominal section spacing (0.4 cm).

The pathologists also measured the maximum linear size in the anterior-posterior (AP) and superior-inferior (SI) dimensions using the measuring tools in Sedeen and, for the medial–lateral (ML) dimension, multiplied the number of sections in which invasive disease was seen by 0.4 cm. The WMSS T-size was identified as the largest of these three measurements for the largest invasive focus, in alignment with CAP/ASCO guidelines for tumor size and included strands of invasive disease radiating away from the tumor [5].

After a minimum 2 week washout period, the pathologists similarly measured SCS T-size, from the SCS images accessing the gross description and simulated grossing diagrams as needed.

In cases where the pathologists expressed difficulty in differentiating between a diagnosis of invasive carcinoma versus in situ disease in one of the formats (WMSS or SCS), the glass slides were used to provide increased detail. In these cases, to reduce bias, the glass slides were also made available for the assessment performed using the other format. The assignment of tumors as unifocal or multifocal was established in earlier work using this sample set [11], and that definition of focality was retained in this study.

### Image analysis and assessment of secondary metrics

For comparison with volume directly measured from WMSS in each case, tumor volume was calculated from the maximum linear sizes (in AP, SI, ML) measured from WMSS and assuming ellipsoidal tumor shape [26, 28].

Four secondary metrics were defined to help explain observed relationships between the primary metrics for tumor size.

Two surrogates for tumor sampling were estimated to describe the influence of format (SCS versus WMSS). First, the '(% sampled)', was defined as the fraction of total invasive tumor area sampled (outlined in the SCS) relative to that outlined in the WMSS. Second, the WMSS overlaid with the virtual samples were inspected in Sedeen to determine whether the maximum linear size of the invasive tumor was fully captured. Undersampling was deemed to have occurred if any contoured tumor region used in the measurement of WMSS T-size extended beyond the overlaid, virtual samples.

Third, to describe the influence of 'compactness' or cellularity, a five-point tumor border index (BI) was devised to subjectively parametrize 3D tumor shape (Fig. 1). The BI was estimated from WMSS in each case. The endpoints of the BI scale characterize an extensively diffuse, infiltrative pattern throughout both the tumor interior and border admixed with normal elements (BI = 1), versus a well-localized invasive mass with a smooth or regular border (BI = 5, high cellularity). Intermediate values characterize tumors that appear moderately diffuse with infiltration of normal elements concentrated at the tumor borders rather than interior (BI = 2), and tumors deemed to have extensive or moderate irregularity or deviation from a smooth border (BI = 3,4).

Fourth, to parametrize discordance in T-size measurements between the two formats, the '(% difference)' was calculated as follows: (WMSS T-size-SCS T-size)/WMSS T-size × 100%.

### Statistical analysis

For the primary outcomes, difference testing between WMSS T-size and SCS T-size was performed using the paired *t*-test after verifying normality for both datasets. The Spearman rank-order correlation coefficient was calculated to assess correlation between WMSS T-size and WMSS tumor volume.

For the secondary outcomes, The Spearman rank-order correlation coefficient was applied to assess whether more diffuse tumors are associated with undersampling compared to more compact ones [comparing BI and (% sampled)] and to assess the role of undersampling in discordant T-size between WM and SCS (comparing % sampled) and (% difference). The nonparametric test was used in the latter comparison after logarithmic transformation failed to normalize the datasets. Difference testing between (ellipsoid) calculated and (WMSS) directly-measured tumor volume was performed using the paired *t*-test after normalizing both right-skewed distributions with a cube-root transformation. All statistical tests were performed using R (Version x64 3.2.1; R Development Core Team; The R Foundation for Statistical Computing; Vienna, Austria).

## Results

### Comparison of WMSS and SCS measurements of T-size

#### Primary metrics

A highly significant difference ($p < 0.001$) was observed between T-size obtained using WMSS versus SCS

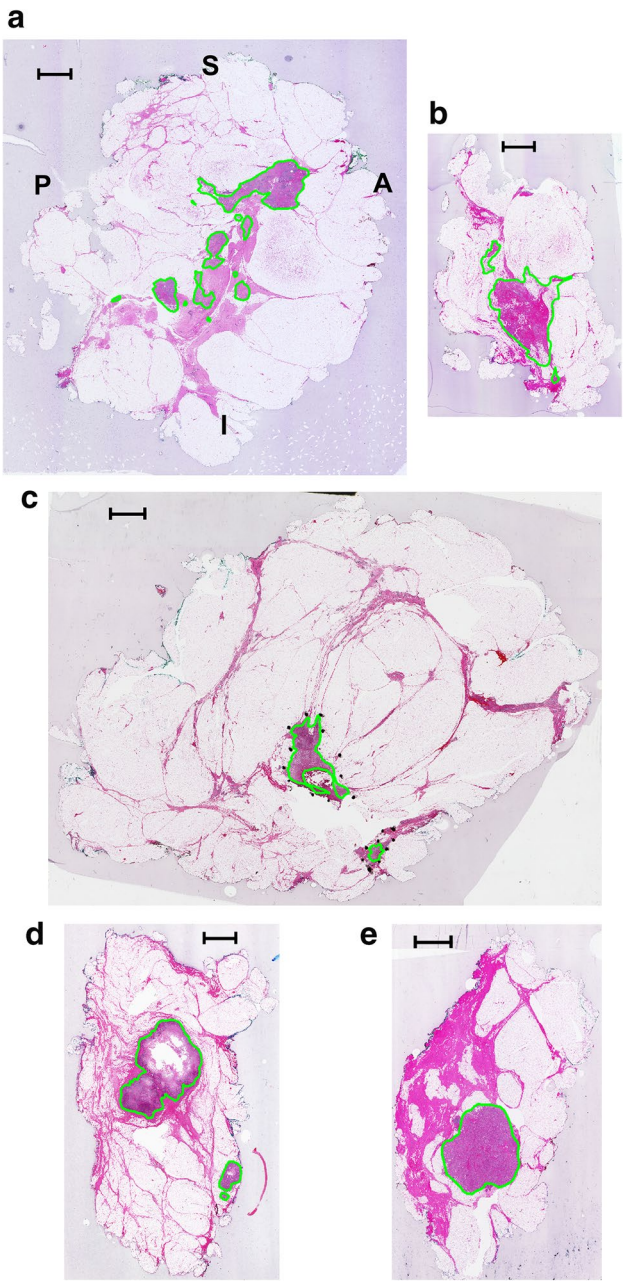


**Fig. 1** Examples characterizing border index (BI): **a** extensively diffuse, BI = 1; **b** moderately diffuse, BI = 2; **c** extensively irregular border, BI = 3; **d** moderately irregular border, BI = 4; **e** regular border, BI = 5. Invasive disease is enclosed in the green contours. Image orientation for all images is as shown in **a**. Scale bar = 5 mm; *A* anterior, *P* posterior, *S* superior, *I* inferior

[means = (2.34 cm; 1.99 cm)]. In the majority of the study cases (61.8%, 34/55), WMSS yielded a higher estimate of T-size compared to SCS.

In 16.4% of the cases (9/55), the TNM staging was changed when T-size was measured with WMSS instead of SCS. In the majority of these cases, the WMSS T-size measurement 'upstaged' the tumor from T1 to T2 relative to SCS measurement (7/9 cases), and, in one case, from T2 to T3. In one case, WMSS measurement shifted the T-size from Tis, as obtained in SCS, to T1 by visualization of micrometastatic deposits that were not sampled in SCS.

Concordant T-size between WMSS and SCS was observed in 38.2% (21/55) of cases. There was no case in which the SCS T-size exceeded WMSS T-size.

### Secondary metrics

Invasive carcinoma was not entirely sampled by SCS technique in 70.6% of the discordant cases (24/34), and in 14.3% (3/21) of the cases where T-size was concordant between the two formats.

No statistically significant correlation between (% sampled) and (% difference) was detectable for the present sample size ($r = -0.163$, $p = 0.235$). However, a low positive correlation was observed between (% sampled) and BI ($r = 0.464$, $p < 0.001$) (Fig. 2a), with a moderate tendency for more compact tumors to be sampled more extensively. The distribution of BI for the study set is shown in Fig. 2b.

Two examples illustrating how the conventional sampling procedure can yield smaller T-size measurements are shown in Fig. 3. In Fig. 3a–c, SCS does not fully capture the dimension with the largest tumor size, which identified as the plane of sectioning only with WMSS. Figure 3d–f exemplifies underestimation of T-size occurring when the maximum size is seen to occur in the same dimension (ML) in both formats, but not fully captured in SCS. Sampling has a similar effect on both in-plane and ML assignments of T-size. The proportion of tumors with T-size under-sampled in ML versus SI/AP dimensions (70.8% (17/24) ML; 29.2% (7/24) AP/SI) approximately aligns with the proportion of tumors with T-size occurring in those dimensions (67.3% (37/55) ML; 32.7% (18/55) AP/SI).

## Comparison of linear and volumetric measurements of tumor size

### Primary metrics

The distribution of tumor volume is shown in Fig. 4a. A high positive correlation was observed between linear and volumetric tumor size ($r = 0.838$, $p < 0.001$) (Fig. 4b). Figure 4b illustrates the variability in tumor volume with T-size.

### Secondary metrics

Greater variability in tumor volume at a given T-size was observed when there was also variability in BI. One example of this relationship is shown in Fig. 5: different volumes were calculated for two tumors with constant T-size = 3.2 cm. The

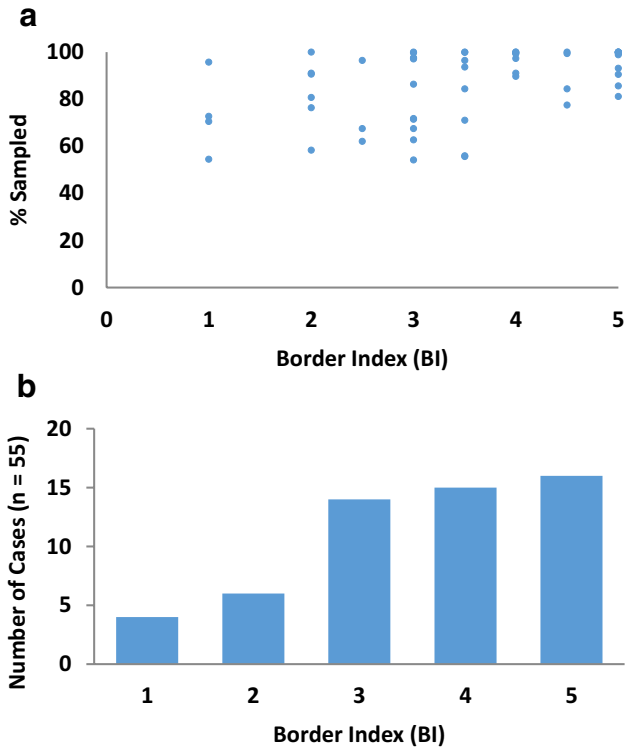


**Fig. 2** **a** Correlation between border index (BI) and the percentage of invasive tumor that is captured in virtual sampling (% sampling) ($r=0.464$, $p<0.001$) for $n=55$ cases. **b** Distribution of BI in sample set

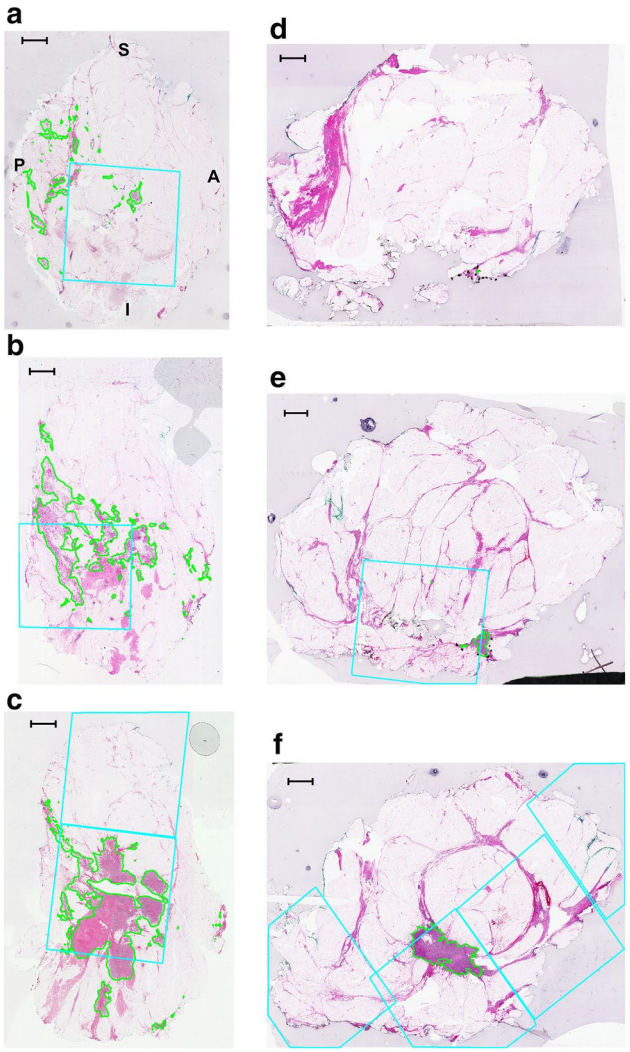


**Fig. 3** Two examples of undersampling responsible for discordant T-size between assessments by WMSS and SCS: Selected WM sections are shown from two cases, the first case in (**a–c**), and the second, in (**d–f**). Invasive tumor is contoured in green and virtual samples are delineated in cyan. In both cases, sections are shown at 2.0 cm (**a**, **d**), 2.8 cm (**b, e**) and 3.6 cm (**c, f**) from the medial aspect. In the first case, the maximum linear size was deemed to occur in the AP dimension in WMSS (T-size = 5.48 cm), but in ML with SCS (T-size = 2.8 cm) because the full extent of invasive tumor was not sampled in the plane of the sections (green contours lying outside the cyan boxes in **a** and **b**). In the second case, although the maximum size was deemed to occur in the ML dimension in both formats, it was underestimated in SCS because the invasive tumor seen at the medial (**d**) and lateral (4.0 cm from medial aspect, not shown) aspect in WMSS was not captured in SCS (WMSS, SCS T-size = 2.8 cm; 2.0 cm). The % of tumor area sampled, % difference between WMSS and SCS T-size measurements, and border index are (70.5%, 48.9%, 1), (67.5%, 28.6%, 2.5) respectively for the (first, second) cases. Image orientation for all images is as shown in **a**). Scale bar = 5 mm; *A* anterior, *P* posterior, *S* superior, *I* inferior

lesser volume was calculated from the more diffuse tumor (Fig. 5a–c; 1.30 $cm^3$; BI = 2), and the greater volume from the more compactly distributed tumor(Fig. 5d–f; 7.58 $cm^3$, BI = 3.5).

Tumor volumes reported directly from WMSS were significantly lower than those calculated using ellipsoid modeling [$p<0.001$, mean values = (1.18 $cm^3$; 1.45 $cm^3$)].

## Discussion

In a recent pilot study distinctive tumor growth patterns were associated with the main pathologic subtypes of breast cancer. Such patterns could potentially inform surgical planning to reduce risk of an involved margin [27]. A larger study found that tumors with ellipsoidal shape were associated with more aggressive phenotypes, compared with spherical lesions [28].

This study explores two alternative, 3-D representations of tumor size: WMSS T-size and volume. To our knowledge this is the first report of primary tumor measurement unbiased by sampling and sparse sectioning. The approach to volume measurement was not restricted to a pre-determined geometric model and therefore permitted

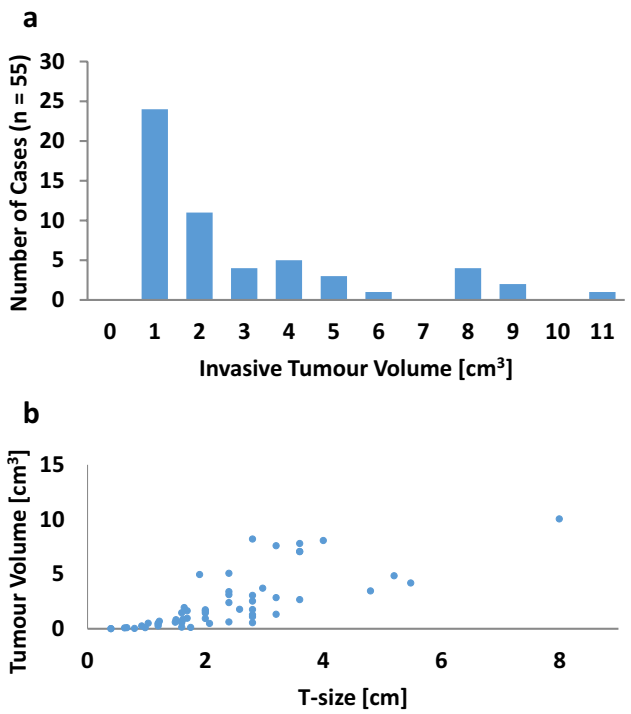


**Fig. 4** **a** Distribution of tumor volume directly measured from WMSS (mean, median values = 2.34 $cm^3$, 1.43 $cm^3$). **b** Correlation between WMSS T-size and volume ($r = 0.84$, $p < 0.001$)

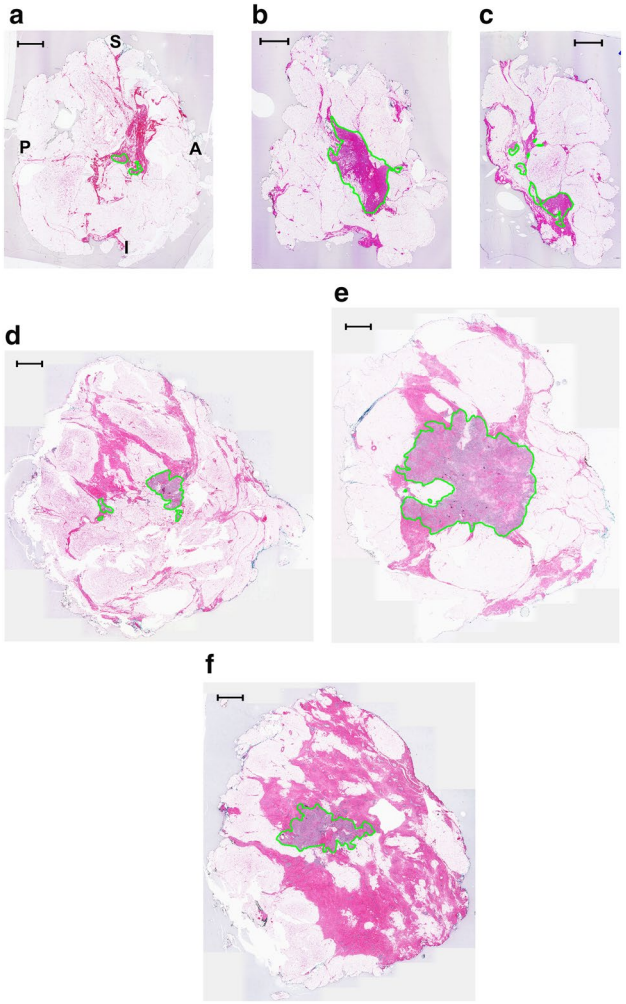


**Fig. 5** Variability in tumor volume for constant T-size: Selected whole-mount sections from two cases are shown. In the first case (**a**–**c**), sections are shown at **a** 2.8 cm, **b** 3.6, and **c** 4.4 cm from the medial aspect. In the second case (**d**–**f**), sections are shown at **d** 4.0 cm, **e** 5.2, and **f** 6.4 cm from the medial aspect. In both cases the maximum linear size is measured to be 3.2 cm in the ML dimension, since, in both cases, tumor was detected in 8 serial sections (8 sections × 0.4 cm spacing between sections section = 3.2 cm). However the tumor volume is 1.30 $cm^3$ in the first case, and 7.58 $cm^3$ in the second; border index = (2, 3.5). Image orientation for all images is as shown in **a**). Scale bar = 5 mm; *A* anterior, *P* posterior, *S* superior, *I* = inferior

inclusion of the whole tumor distribution, even if discontinuous. While the WMSS methodology is resource-intensive, these unbiased measurements could also be estimated from tissue sections prepared using conventional histology equipment if specimens are exhaustively sampled.

T-size estimates from WMSS were significantly larger than conventional ones. There was visual evidence of undersampling in SCS in the majority of discordant cases. Undersampling tended to occur more frequently in more diffuse tumors than in compact ones. There was a strong positive correlation between T-size and volume, measuring both from WMSS. This suggests that at least for this sample set, linear size measured from WMSS is a reasonable surrogate for tumor burden.

## Comparison of WMSS and SCS measurements of T-size

Although the majority of discordances in WMSS and SCS T-size were attributable to undersampling, it was not identified in 10 (out of the 34) discordant cases. In 7/10 cases, discrepancy in SCS T-size occurring in AP or SI dimensions was introduced when summing measurements over multiple SCS that were separated by small gaps after reassembly. This effect must be considered if unbiased estimates of T-size and volume are taken from exhaustive, conventional sampling and histology processing rather than WMSS techniques. In the remaining three cases, discrepancy was attributed to observer variability since areas were sampled in SCS but not detected by observers. In two occurrences, the 'misses' were micrometastases or small satellites, while the third was a larger ($1.4 \times 3.9$ $mm^2$) area of invasive lobular carcinoma.

The (% sampled) and (% difference) were uncorrelated. Contributing to this observation were those cases where

a very small but distant tumor region was missed. When occurring at the ML margin, this effect produced an automatic increase in (% difference) corresponding to 0.4 cm, but with negligible change in (% sampled). Technical challenges associated with sampling more diffuse or impalpable tumors may underlie these 'misses'.

These results highlight the impact of increasing coverage with WMSS on T-size measurement; sampling by SCS did not achieve full coverage of the tumor in 27/55 cases, leading to discordant T-size measurement in 24 of these occurrences. Earlier studies motivated by limitations of conventional sampling indicate more reliable tumor size measurements with large-format or WM sections in 8.8–37% of cases [29–31]. Earlier studies have also leveraged WM to identify tumor distribution, and associate diffuse patterns with a poorer prognosis [32–34]. Strength of the present study is the inclusion of serial sectioning, digital techniques, and a design which enables both assessments to be performed on each patient.

## Comparison of linear and volumetric measurements of tumor size

Variability in volume for constant T-size may occur because, unlike T-size, volume is unaffected by the presence of any intervening normal tissue or non-invasive disease.

We observed substantial variability in tumor volume for constant T-size and this was reflected in substantial differences in the rankings of T-size and volume. For 30 cases, T-size rank was higher than for volume while in 20 cases volumetric rank exceeded linear; for five cases the ranks were identical. This variability may result from variations in 'compactness' or cellularity of tumors as parametrized by the 'border index'. The high, positive correlation between linear and volumetric size in this study may reflect the weighting of the sample set toward more compact, higher-BI tumors (Fig. 4a). This positive correlation is consistent with results from previous studies that were based on ellipsoid geometry, despite the use of more precise, WMSS methodologies here [35]. However, we have also demonstrated that WMSS methodology yields significantly smaller volumes compared with the ellipsoid model, suggesting a complex interplay of variables underlie the relationship between linear and volumetric tumor size.

There are two key limitations to this study. First, tumor area, assigned at the top of the block, is assumed to be constant through the 0.4 mm thickness (ML direction) of each block, and tumor volume is calculated as a function of area (and thickness). If tumor area varies through the block, then WMSS may poorly represent the true volume of tumor cells. It is assumed that such errors effectively balance each other in the 'snapshots' taken at every 0.4 cm through the tumor in the ML dimension. Second, the planes in which the maximum size can be identified for T-size assessment are constrained to the plane of sectioning (capturing AP and SI) and the direction of sectioning (ML). In reality, the maximum size of invasive tumor may occur in an oblique plane and cannot be captured without more high-resolution volume rendering (and more exhaustive sectioning). Limitations of the virtual sampling approach as a model for real sampling are detailed elsewhere [11].

We have demonstrated that significantly larger T-size is measured using WMSS compared with conventional histologic sampling, usually resulting from undersampling in the latter. Although volumetric and linear tumor sizes are highly correlated, this study illustrates that for a given T-size the tumor volume can vary markedly.

While tumor biology probably provides the most important prognostic and predictive information, tumor size remains an important determinant of outcome. More precise, 3-D measures of tumor size have the potential to improve estimation of prognosis and accurately prescribe therapies according to risk. Obtaining those measures through high-resolution, volumetric breast imaging modalities (e.g., automatic breast ultrasound and magnetic resonance imaging) could help plan more effective primary treatments. The large-format 3-D histology provided by WMSS is an ideal method for validation of such imaging.

The presentation of tumor cellularity, especially in the neoadjuvant setting, motivates the development of more rigorous, unbiased descriptors in future studies. Larger studies are needed to test the relationships between alternative measurements of tumor size and clinical outcomes including nodal involvement, and locoregional or distant recurrence.

**Acknowledgements** The authors are grateful to Ms Anoma Gunasekara for her assistance with recruitment, and together with Ms Yulia Yerofeyeva with organizing all aspects of the study logistics and patient tracking. Finally we acknowledge the co-operation of pathologist assistants Ms Anna-Marie Moskaluk, Mr Ian Cooper. Dr Laibao Sun and Dr Peter Leventis for performing the virtual sampling and overseeing the research protocol, and Adebayo Adeeko for assistance with specimen preparation.

**Funding** This work was supported by the Canadian Breast Cancer Research Alliance/Canadian Cancer Society Research Institute.

**Data Availability** The datasets created and analyzed during the current study are available from the corresponding author on reasonable request.

## Compliance with ethical standards

**Conflict of interest** The authors do not have a conflict of interest.

**Ethical approval** This study was conducted in full compliance with the applicable, current Canadian law.

## References


1. Fisher B, Slack NH, Bross ID (1969) Cancer of the breast: size of neoplasm and prognosis. Cancer 24:1071–1080
2. Tabar L, Vitak B, Chen HH et al (2000) The Swedish Two-County Trial twenty years later. updated mortality results and new insights from long-term follow-up. Radiol Clin N Am 38:625–651
3. Leitner SP, Swern AS, Weinberger D et al (1995) Predictors of recurrence for patients with small (one centimeter or less) localized breast cancer (T1a,b N0 M0). Cancer 76:2266–2274
4. Koscielny S, Tubiana M, Le MG et al (1984) Breast cancer: relationship between the size of the primary tumour and the probability of metastatic dissemination. Br J Cancer 49:709–715
5. Amin M, Edge S, Greene F et al (2017) AJCC cancer staging manual, 8th edn. Springer, Chicago
6. Carter CL, Allen C, Henson DE (1989) Relation of tumor size, lymph node status, and survival in 24,740 breast cancer cases. Cancer 63:181–187
7. Koscielny S, Tubiana M, Lê MG et al (1984) Breast cancer: relationship between the size of the primary tumour and the probability of metastatic dissemination. Br J Cancer 49:709–715
8. Smart CR, Myers MH, Gloeckler LA (1978) Implications from SEER data on breast cancer management. Cancer 41:787–789
9. Lester S, Bose S, Chen Y-Y et al (2013) Protocol for the examination of specimens from patients with invasive carcinoma of the breast protocol applies to all invasive carcinomas of the breast, including ductal. Arch Pathol Lab Med 133(10):1515–1538
10. Graham R, Homer MJ, Katz J et al (2002) The pancake phenomenon contributes to the inaccuracy of margin assessment in patients with breast cancer. Am J Surg 184:89–93
11. Clarke GM, Holloway CMB, Zubovits JT et al (2016) Whole-mount pathology of breast lumpectomy specimens improves detection of tumour margins and focality. Histopathology 69:35–44. https://doi.org/10.1111/his.12912
12. Michaelson JS, Silverstein M, Wyatt J et al (2002) Predicting the survival of patients with breast carcinoma using tumor size. Cancer 95:713–723. https://doi.org/10.1002/cncr.10742
13. Hofmeyer S, Pekár G, Gere M et al (2012) Comparison of the subgross distribution of the lesions in invasive ductal and lobular carcinomas of the breast: a large-format histology study. Int J Breast Cancer 2012:436141. https://doi.org/10.1155/2012/436141
14. Dekker TJA, van de Velde CJH, van Pelt GW et al (2013) Prognostic significance of the tumor-stroma ratio: validation study in node-negative premenopausal breast cancer patients from the EORTC perioperative chemotherapy (POP) trial (10854). Breast Cancer Res Treat 139:371–379. https://doi.org/10.1007/s10549-013-2571-5
15. Downey CL, Simpkins SA, White J et al (2014) The prognostic significance of tumour-stroma ratio in oestrogen receptor-positive breast cancer. Br J Cancer 110:1744–1747. https://doi.org/10.1038/bjc.2014.69
16. Moorman AM, Vink R, Heijmans HJ et al (2012) The prognostic value of tumour-stroma ratio in triple-negative breast cancer. Eur J Surg Oncol 38:307–313. https://doi.org/10.1016/j.ejso.2012.01.002
17. Guth U, Brenckle D, Huang DJ et al (2009) Three-dimensional pathological size assessment in primary breast carcinoma. Breast Cancer Res Treat 116:257–262
18. Kerr KM, Lamb D (1988) A comparison of patient survival and tumour growth kinetics in human bronchogenic carcinoma. Br J Cancer 58:419–422
19. Tsai CH, Lin CM, Hsieh CC et al (2006) Tumor volume is a better prognostic factor than greatest tumor diameter in stage Ia non-small cell lung cancer. Thorac Cardiovasc Surg 54:537–543
20. Mai KT, Mokhtar G, Burns BF et al (2003) A simple technique for calculation of the volume of prostatic adenocarcinomas in radical prostatectomy specimens. Pathol Res Pr 199:599–604
21. Clarke GM, Murray M, Holloway CMB et al (2012) 3D pathology volumetric technique: a method for calculating breast tumour volume from whole-mount serial section images. Int J Breast Cancer 2012:691205. https://doi.org/10.1155/2012/691205
22. Sun L, Wang D, Zubovits JT et al (2009) An improved processing method for breast whole-mount serial sections for three-dimensional histopathology imaging. Am J Clin Pathol 131:383–392. https://doi.org/10.1309/AJCPVBZZ4IKJHY3U
23. Clarke GM, Eidt S, Sun L et al (2007) Whole-specimen histopathology: a method to produce whole-mount breast serial sections for 3-D digital histopathology imaging. Histopathology 50:232–242. https://doi.org/10.1111/j.1365-2559.2006.02561.x
24. Clarke GM, Peressotti C, Constantinou P et al (2010) Increasing specimen coverage using digital whole-mount breast pathology: implementation, clinical feasibility and application in research. Comput Med Imaging Graph 35:531–541. https://doi.org/10.1016/j.compmedimag.2011.05.002
25. Clarke GM, Zubovits JT, Katic M et al (2007) Spatial resolution requirements for acquisition of the virtual screening slide for digital whole-specimen breast histopathology. Hum Pathol 38:1764–1771. https://doi.org/10.1016/j.humpath.2007.04.006
26. Wapnir IL, Wartenberg DE, Greco RS (1996) Three dimensional staging of breast cancer. Breast Cancer Res Treat 41:15–19
27. Merrill AL, Buckley J, Tang R et al (2016) A study of the growth patterns of breast carcinoma using 3D reconstruction: a pilot study. Breast J. https://doi.org/10.1111/tbj.12688
28. Moon HG, Kim N, Jeong S et al (2015) The clinical significance and molecular features of the spatial tumor shapes in breast cancers. PLoS ONE 10:1–14. https://doi.org/10.1371/journal.pone.0143811
29. Jackson PA, Merchant W, McCormick CJ, Cook MG (1994) A comparison of large block macrosectioning and conventional techniques in breast pathology. Virchows Arch 425:243–248
30. Foschini MP, Baldovini C, Ishikawa Y, Eusebi V (2012) The value of large sections in surgical pathology. Int J Breast Cancer 2012:785947. https://doi.org/10.1155/2012/785947
31. Foster MR, Harris L, Biesemier KW (2012) Large format histology may aid in the detection of unsuspected pathologic findings of potential clinical significance: a prospective multiyear single institution study. Int J Breast Cancer 2012:532547. https://doi.org/10.1155/2012/532547
32. Tot T (2003) The diffuse type of invasive lobular carcinoma of the breast: morphology and prognosis. Virchows Arch 443:718–724. https://doi.org/10.1007/s00428-003-0881-4
33. Tot T (2007) Clinical relevance of the distribution of the lesions in 500 consecutive breast cancer cases documented in large-format histologic sections. Cancer 110:2551–2560. https://doi.org/10.1002/cncr.23052
34. Tot T (2016) Diffuse invasive breast carcinoma of no special type. Virchows Arch 468:199–206. https://doi.org/10.1007/s00428-015-1873-x
35. Güth U, Brenckle D, Huang DJ et al (2009) Three-dimensional pathological size assessment in primary breast carcinoma. Breast Cancer Res Treat 116:257–262. https://doi.org/10.1007/s10549-008-0115-1

## Affiliations

**G. M. Clarke[1] · C. M. B. Holloway[2,3] · J. T. Zubovits[4,5] · S. Nofech-Mozes[4,6] · M. Murray[7] · K. Liu[8] · D. Wang[8] · A. Kiss[9,10] · M. J. Yaffe[11,12]**

G. M. Clarke
gclarke.sri@gmail.com

C. M. B. Holloway
claire.holloway@sunnybrook.ca

J. T. Zubovits
jzubovits@rougevalley.ca

S. Nofech-Mozes
Sharon.nofech-mozes@sunnybrook.ca

M. Murray
mayanmurray@gmail.com

K. Liu
kela.liu@sunnybrook.ca

D. Wang
dan.wang@sunnybrook.ca

A. Kiss
alex.kiss@ices.on.ca

1 Physical Sciences Platform, Sunnybrook Research Institute, Room C7-27c 2075 Bayview Avenue, Toronto, ON M4N 3M5, Canada

2 Department of Surgery, Faculty of Medicine, University of Toronto, Toronto, Canada

3 Department of Surgery, Sunnybrook Health Sciences Centre, Room T2-015 2075 Bayview Avenue, Toronto, ON M4N 3M5, Canada

4 Department of Laboratory Medicine and Pathobiology, Faculty of Medicine, University of Toronto, Toronto, Canada

5 Present Address: Department of Pathology, Scarborough and Rouge Hospital, 3030 Birchmount Road, Toronto, ON M1W 3W3, Canada

6 Sunnybrook Health Sciences Centre, Room E423a 2075 Bayview Avenue, Toronto, ON M4N 3M5, Canada

7 Physical Sciences Platform, Sunnybrook Research Institute, Room C7-48a 2075 Bayview Avenue, Toronto, ON M4N 3M5, Canada

8 Physical Sciences Platform, Sunnybrook Research Institute, Room C7-27a 2075 Bayview Avenue, Toronto, ON M4N 3M5, Canada

9 Research Design and Biostatistics, Sunnybrook Research Institute, Toronto, ON, Canada

10 Institute of Health Policy, Management and Evaluation, University of Toronto, Room G106 2075 Bayview Avenue, Toronto, ON M4N 3M5, Canada

11 Departments of Medical Biophysics and Medical Imaging, Faculty of Medicine, University of Toronto, Toronto, Canada

12 Physical Sciences Platform, Sunnybrook Research Institute, Room S6-57 2075 Bayview Avenue, Toronto, ON M4N 3M5, Canada